Vol. 17 No. 2 (2026) 64-71

Jurnal Riset
Teknologi Pencegahan Pencemaran
Industri

Journal homepage: https://www.jrtppi.id

Spatial Modeling of Tailings-Associated Metal(loid)s and Surface-Water Quality in the Ajkwa River Basin, Mimika Regency, Central Papua, Indonesia

Obed Patiung*, Mapuay Menasye Theo Afasedanya, Abd. Rahim

Mining Engineering, Politeknik Amamapare

ARTICLE INFO

Article history:

Received January 04 2026

Received in revised form March 20, 2026

Accepted April 20, 2026

Available online November 19, 2026

Keywords:

Mine Tailings

Sediment Geochemistry

Spatial Modeling

Inverse Distance Weighting

Ajkwa River

ABSTRACT

Large-scale copper-gold mining in Mimika generates tailings that interact with the Ajkwa River system and may influence aquatic geochemistry. This study integrated paired water-sediment sampling, laboratory metal(loid) analysis, censor-aware interpretation of non-detect water data, and spatial modeling. Twenty paired surface-water and sediment samples were collected at identical coordinates. In-situ pH and dissolved oxygen (DO) were measured, while water Cu, As, and Hg were analyzed by atomic absorption spectrometry and sediment Cu and As by X-ray fluorescence. Water pH ranged from 7.49 to 7.78 and DO from 5.41 to 6.59 mg L−1. All water-phase metals were below laboratory reporting limits with no RL-based exceedance of the relevant Class III/IV criteria. Sediment Cu ranged from 805.74 to 1,644.79 mg kg−1 and As from 104.62 to 471.55 mg kg−1. IDW cross-validation showed stronger performance for As (R^2 = 0.965; RMSE = 22.25; MAE = 16.05 mg kg−1) than Cu (R^2 = 0.391; RMSE = 148.73; MAE = 86.10 mg kg−1). The interpolated surfaces represent model estimates, not direct measurements. All sediment Cu and As values exceeded freshwater PECs, but these represent screening-level indications rather than formal ecological risk. The findings support sediment-focused monitoring and validated spatial assessment in the Ajkwa River Basin.

Keywords: Mine Tailings; Sediment Geochemistry; Spatial Modeling; Inverse Distance Weighting; Ajkwa River.

*Correspondence author.
E-mail: obedpatiung85@gmail.com (Obed Patiung)

doi: https://doi.org/10.21771/jrtppi.2026.v17.no2.p64-71
2503-5010/2087-0965© 2026 Jurnal Riset Teknologi Pencegahan Pencemaran Industri-BBSPJPPI (JRTPPI-BBSPJPPI).
This is an open acces article under the CC BY-NC-SA license (https://creativecommons.org/licenses/by-nc-sa/4.0/).
Accreditation number: (Ristekdikti) 158/E/KPT/2026

INTRODUCTION

Mine tailings can act as long-term sources of potentially toxic metal(loid)s, with environmental impacts shaped by mineralogy, hydrology, particle size, redox conditions, and contaminant retention or remobilization (Granger et al., 2022; Kolarova & Napiórkowski, 2021). Sediments can retain spatially heterogeneous metal loads influenced by texture, organic matter, and depositional processes (Nazir et al., 2024). They also function as sinks and secondary contaminant sources, depending on speciation, mineral hosts, grain size, redox conditions, and bioavailability (Luoma, 1983; Rainbow, 2007; Väänänen et al., 2018). Metal(loid)s stored in sulfides, Fe/Mn oxides, and other reactive phases may be remobilized under changing geochemical conditions (Doherty et al., 2021; Lee et al., 2010; Toevs et al., 2006). Spatial variability in mining-affected rivers may reflect source proximity, particle sorting, hydrodynamics, and depositional processes (Cuevas et al., 2023; Granger et al., 2022; Tian et al., 2024). Metal(loid)s may also persist over substantial distances according to particle and geochemical characteristics (Cuevas et al., 2023; Doherty et al., 2021).

The Ajkwa River system in Mimika Regency, Central Papua, is influenced by one of the world's largest copper-gold mining districts. Previous studies have documented mining-related riparian and coastal disturbance (Alonzo et al., 2016) as well as ecosystem changes associated with acid mine drainage and tailings/non-tailings materials in the ModADA sedimentation area (Taberima et al., 2020). However, a paired water-sediment framework that simultaneously distinguishes censored water-phase observations from measured sediment concentrations and validates spatial interpolation performance remains limited. GIS can support contaminant mapping between discrete sampling stations, but interpolation method, sampling density, and parameter selection can substantially affect prediction uncertainty (Qiao et al., 2018; Wen et al., 2022).

Recent geospatial studies further emphasize the importance of accounting for spatial heterogeneity and validating model or remotely sensed outputs to reduce prediction errors and false positives (Jewell et al., 2024; Yang & Jia, 2024). Another methodological concern is the treatment of non-detect laboratory data, because substituting censored values with zero or fixed fractions of detection limits can distort descriptive statistics and spatial patterns (Helsel, 2006). Accordingly, this study integrates paired water-sediment measurements, censor-aware interpretation of water-phase Cu, As, and Hg, and cross-validated spatial modeling of sediment Cu and as to characterize environmental patterns, evaluate uncertainty, and distinguish measured geochemical gradients from reporting-limit effects and model-derived surfaces.

METHODS

Study area and sampling design

Field sampling was conducted on 19 June 2026 in the Ajkwa River Basin, Mimika Regency, Central Papua, using purposive sampling. Twenty paired water (A01-A20) and sediment (S01-S20) stations were established at identical coordinates. Water was sampled at 0.30-0.50 m depth, while sediment represented surface tailings/sandy material. Coordinates were projected to WGS 84 / UTM Zone 53S (EPSG:32753), and spatial modeling was restricted to the sampled river corridor.

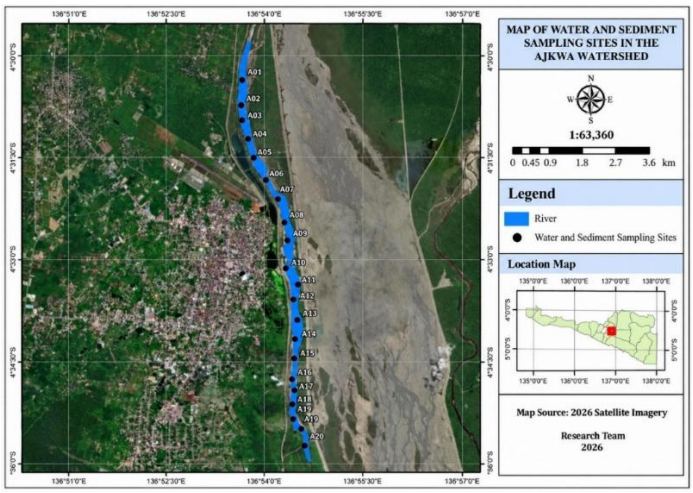


Figure 1. Sampling locations of the 20 paired water-sediment stations in the Ajkwa River corridor. The plot is coordinate-based and does not represent a formal watershed boundary

Field measurements and laboratory analysis

At each water station, pH and dissolved oxygen (DO) were measured in situ, while Cu, As, and Hg were analyzed by AAS at PT SUCOFINDO Makassar Branch. EPA Methods 200.9 and 245.1 were used only as methodological reference points because laboratory certificate numbers, instrument details, and SOP identifiers were unavailable (U.S. Environmental Protection Agency, 1994a, 1994b). Sediment Cu and As were analyzed by XRF at the Mining Engineering Laboratory, Universitas Hasanuddin, with SW-846 Method 6200 as a technical reference (U.S. Environmental Protection Agency, 2007). Sediment Hg data were unavailable. Because detailed QA/QC documentation was not available, no analytical procedures beyond those explicitly documented were inferred.

Reporting limits, censored data, and water-quality benchmarks

All water Cu, As, and Hg concentrations were below laboratory reporting limits (RLs): 0.01-0.02 mg L−1 for Cu, 0.001-0.002 mg L−1 for As, and 0.0008-0.0009 mg L−1 for Hg. The results were treated as left-censored intervals ($0 \leq C < RL$) without substitution (Helsel, 2006). Screening followed Indonesian Government Regulation No. 22 of 2021 for Class III/IV water-quality criteria (Government of Indonesia, 2021), with interpretation limited to whether the reporting intervals remained below the relevant benchmarks.

Spatial analysis and cross-validation

Spatial processing and IDW interpolation were performed using Python 3.12. Spatial processing used WGS 84 (EPSG:4326) and WGS 84 / UTM Zone 53S (EPSG:32753), with distance-based interpolation performed in UTM coordinates. Quantitative interpolation was limited to sediment Cu and As within the sampled river corridor. IDW parameters were optimized using leave-one-out cross-validation by testing power values of 1.0-3.0 and 3-19 nearest neighbors; the selected model used power = 2.5, six neighbors, and a 50 m grid *based on the lowest LOOCV prediction error* (Qiao et al., 2018; Wen et al., 2022). Model performance was evaluated using RMSE, MAE, ME, and R^2.

Descriptive, exploratory, and sediment-screening analyses

Descriptive statistics included minimum, maximum, mean, median, and standard deviation, while Spearman and Pearson correlations assessed sediment trends and Cu-As co-variation. These analyses describe spatial patterns without implying causal downstream transport. Sediment Cu and As were compared with freshwater PECs of 149 and 33 mg kg−1, respectively (MacDonald et al., 2000). These benchmarks are screening tools rather than site-specific toxicity criteria and should be interpreted alongside bioavailability, sediment chemistry, and biological evidence (Burton, 2002; Väänänen et al., 2018). They do not represent an Indonesian regulatory classification.

RESULT AND DISCUSSION

Sampling characteristics, pH, and dissolved oxygen

The 20 paired stations formed a narrow north-south sampling corridor. Surface-water pH ranged from 7.49 to 7.78, with a mean of 7.60 ± 0.08. DO ranged from 5.41 to 6.59 mg L−1, with a mean of 6.05 ± 0.34 mg L−1. All pH values fell within the Class III/IV range of 6-9, and all DO values exceeded the Class III minimum of 3 mg L−1 and the Class IV minimum of 1 mg L−1. The ordered station sequence shows a general decline in pH after local variation in the first five stations and a general increase in DO after the minimum observed at A02. Because hydrological and tidal covariates were not measured, these patterns are reported descriptively rather than interpreted as effects of tailings.

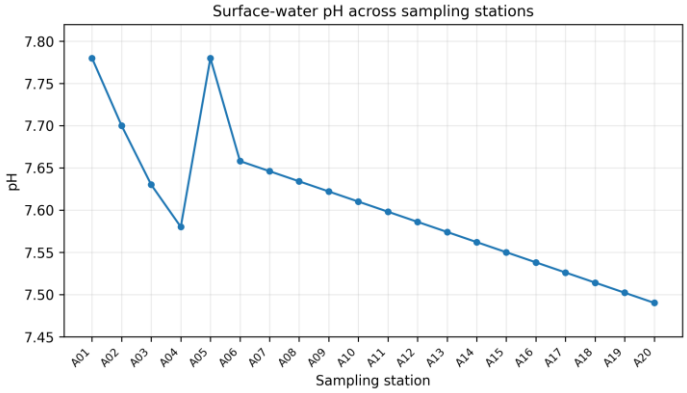


Figure 2. Surface-water pH measured at stations A01-A20

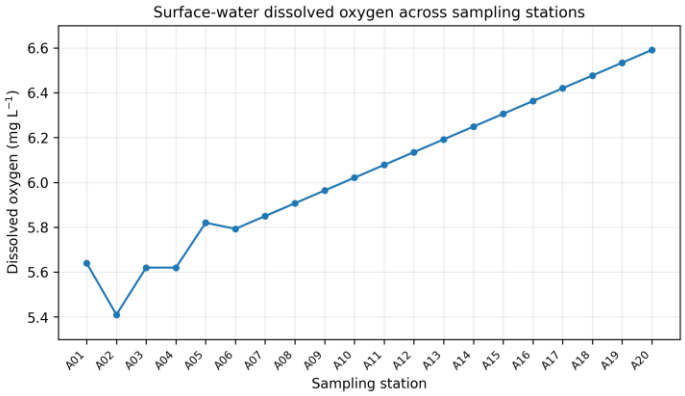


Figure 3. Dissolved oxygen measured at stations A01-A20

Table 1. Coordinates and in-situ surface-water measurements at the 20 paired stations

Station pair	Longitude	Latitude	pH	DO (mg L−1)
A01/S01	136°53'35.393" E	4°30'21.348" S	7.78	5.64
A02/S02	136°53'34.255" E	4°30'43.558" S	7.7	5.41
A03/S03	136°53'34.600" E	4°30'56.935" S	7.63	5.62
A04/S04	136°53'39.884" E	4°31'13.293" S	7.58	5.62
A05/S05	136°53'45.010" E	4°31'30.231" S	7.78	5.82
A06/S06	136°53'55.819" E	4°31'49.555" S	7.658	5.793

A07/S07	136°54'06.632" E	4°32'06.483" S	7.646	5.85
A08/S08	136°54'11.756" E	4°32'27.024" S	7.634	5.907
A09/S09	136°54'13.884" E	4°32'42.484" S	7.622	5.964
A10/S10	136°54'12.032" E	4°33'07.232" S	7.61	6.021
A11/S11	136°54'23.552" E	4°33'21.330" S	7.598	6.078
A12/S12	136°54'18.366" E	4°33'33.966" S	7.586	6.135
A13/S13	136°54'21.694" E	4°33'52.708" S	7.574	6.192
A14/S14	136°54'19.658" E	4°34'09.513" S	7.562	6.249
A15/S15	136°54'18.944" E	4°34'26.308" S	7.55	6.306
A16/S16	136°54'16.611" E	4°34'44.616" S	7.538	6.363
A17/S17	136°54'19.615" E	4°34'53.979" S	7.526	6.42
A18/S18	136°54'17.378" E	4°35'06.857" S	7.514	6.477
A19/S19	136°54'18.091" E	4°35'20.060" S	7.502	6.534
A20/S20	136°54'26.076" E	4°35'28.676" S	7.49	6.591

Cu, As, and Hg in surface water

All water Cu, As, and Hg results were left-censored. Cu was <0.01 mg L−1 at 16 stations and <0.02 mg L−1 at A04, A10, A15, and A19; As was <0.001 mg L−1 at 17 stations and <0.002 mg L−1 at A07, A14, and A19; and Hg was <0.0008 mg L−1 at 16 stations and <0.0009 mg L−1 at A04, A11, A15, and A19. All reporting intervals were within the Class III/IV benchmarks, so no exceedance was demonstrated, although true concentrations cannot be assumed to be zero.

Table 2. AAS results for surface water. All values are left-censored at laboratory reporting limits (RLs)

Station	Cu (mg L−1)	As (mg L−1)	Hg (mg L−1)	Screening vs Class III/IV
A01	<0.01	<0.001	<0.0008	No RL-based exceedance
A02	<0.01	<0.001	<0.0008	No RL-based exceedance
A03	<0.01	<0.001	<0.0008	No RL-based exceedance
A04	<0.02	<0.001	<0.0009	No RL-based exceedance
A05	<0.01	<0.001	<0.0008	No RL-based exceedance
A06	<0.01	<0.001	<0.0008	No RL-based exceedance
A07	<0.01	<0.002	<0.0008	No RL-based exceedance
A08	<0.01	<0.001	<0.0008	No RL-based exceedance
A09	<0.01	<0.001	<0.0008	No RL-based exceedance
A10	<0.02	<0.001	<0.0008	No RL-based exceedance
A11	<0.01	<0.001	<0.0009	No RL-based exceedance
A12	<0.01	<0.001	<0.0008	No RL-based exceedance
A13	<0.01	<0.001	<0.0008	No RL-based exceedance
A14	<0.01	<0.002	<0.0008	No RL-based exceedance
A15	<0.02	<0.001	<0.0009	No RL-based exceedance
A16	<0.01	<0.001	<0.0008	No RL-based exceedance
A17	<0.01	<0.001	<0.0008	No RL-based exceedance
A18	<0.01	<0.001	<0.0008	No RL-based exceedance
A19	<0.02	<0.002	<0.0009	No RL-based exceedance
A20	<0.01	<0.001	<0.0008	No RL-based exceedance

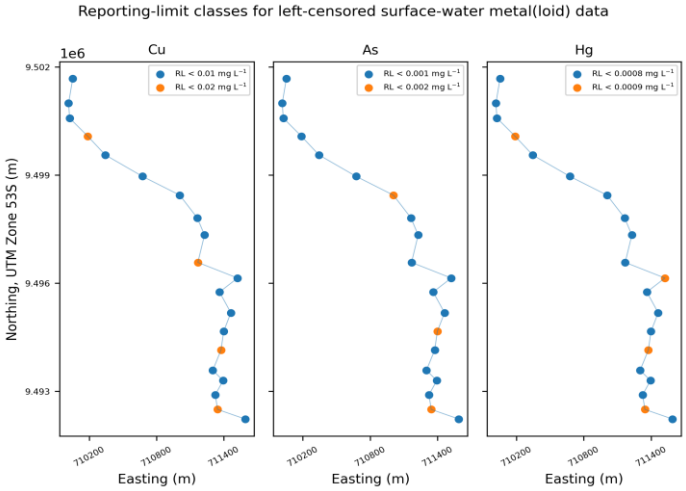


Figure 4. Spatial distribution of reporting limits for water Cu, As, and Hg; symbols indicate thresholds, not concentration gradients.

Cu and As in sediment

Sediment XRF showed greater variability than water-phase data, with Cu ranging from 805.74 to 1,644.79 mg kg−1 (mean 1,064.81 ± 195.61 mg kg−1) and As from 104.62 to 471.55 mg kg−1 (mean 343.94 ± 121.50 mg kg−1). Cu peaked at S07 and reached its minimum at S09, whereas As peaked at S09 and declined to its minimum at S20. These contrasting patterns may reflect differences in sediment texture, mineralogy, organic matter, hydrodynamic sorting, and depositional conditions, as metal(loid) retention varies among Fe/Mn oxides, sulfide minerals, and other reactive phases (Doherty et al., 2021; Lee et al., 2010; Väänänen et al., 2018). However, these mechanisms remain tentative because relevant sediment and hydrodynamic properties were not measured. Along the station sequence, Cu (Spearman ϱ = −0.759, $p < 0.001$) and As (ϱ = −0.854, $p < 0.001$) showed significant negative monotonic trends, while Cu and As were moderately positively associated (Pearson r = 0.532, p = 0.016; Spearman ϱ = 0.612, p = 0.004), indicating partially shared but distinct spatial controls.

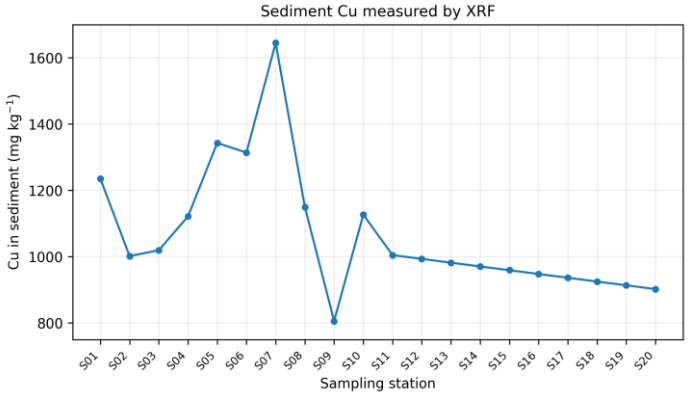


Figure 5. Sediment Cu concentrations measured by XRF at stations S01-S20

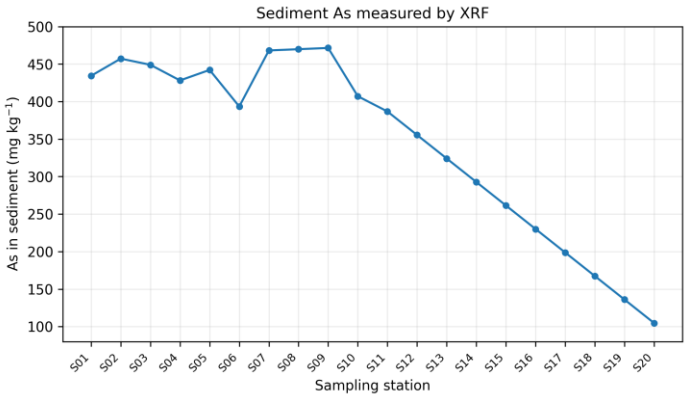


Figure 6. Sediment As concentrations measured by XRF at stations S01-S20

Table 3. Sediment Cu and as measured by XRF. The two station blocks are presented side by side to conserve space. Sediment Hg data were unavailable.

Station	Cu (mg kg−1)	As (mg kg−1)	Station	Cu (mg kg−1)	As (mg kg−1)
S01	1234.97	434.36	S11	1004.66	386.83
S02	1001.70	457.31	S12	993.27	355.47
S03	1019.52	449.06	S13	981.89	324.11
S04	1121.53	428.23	S14	970.51	292.76
S05	1343.06	442.24	S15	959.12	261.40
S06	1313.98	393.47	S16	947.74	230.05
S07	1644.79	468.22	S17	936.35	198.69
S08	1149.65	469.89	S18	924.97	167.33
S09	805.74	471.55	S19	913.59	135.98
S10	1126.88	407.17	S20	902.20	104.62

Sediment IDW performance and spatial surfaces

Leave-one-out cross-validation showed substantially stronger spatial predictability for As than Cu. Cu produced RMSE = 148.73 mg kg−1, MAE = 86.10 mg kg−1, mean error = −14.32 mg kg−1, and R^2 = 0.391, whereas As produced RMSE = 22.25 mg kg−1, MAE = 16.05 mg kg−1, mean error = 0.94 mg kg−1, and R^2 = 0.965. This indicates that the IDW model reproduced the As pattern more consistently, while Cu was affected by strong local variability around S07-S09. Residuals ranged from −446.92 to 366.35 mg kg−1 for Cu and −34.82 to 62.27 mg kg−1 for As, with the largest absolute residuals at S07 for Cu and S06 for As. The small mean errors suggest limited directional bias, while the larger Cu errors confirm weaker predictive performance.

Table 4. Leave-one-out cross-validation metrics for the selected sediment IDW configuration

Analyte	Power	Neighbors	RMSE (mg kg−1)	MAE (mg kg−1)	Mean error (mg kg−1)	R^2
Cu	2.5	6	148.73	86.10	−14.32	0.391
As	2.5	6	22.25	16.05	0.94	0.965

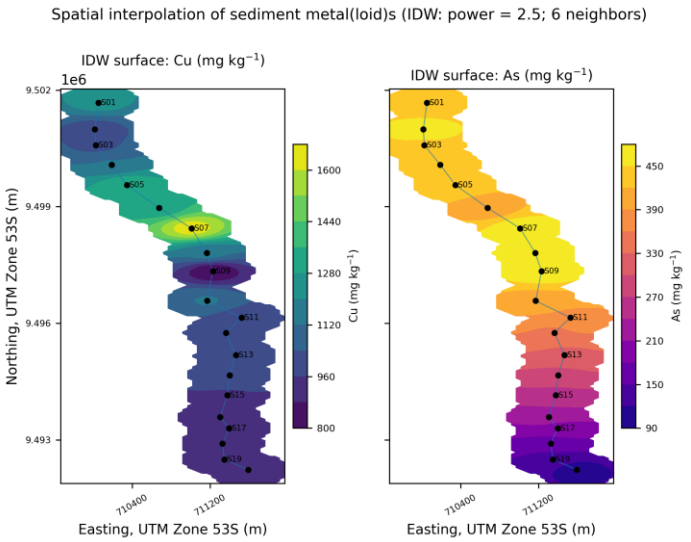


Figure 7. IDW surfaces for sediment Cu and As (power = 2.5; six neighbors), representing model estimates within the sampled corridor

Screening comparison with sediment effect benchmarks

All sediment Cu and As concentrations exceeded freshwater PECs, by 5.4-11.0 times for Cu and 3.2-14.3 times for As. Mean exceedances were approximately 7.1 and 10.4 times, respectively. These results indicate screening-level concern only, not site-specific toxicity or formal ecological risk. The benchmarks do not account for Ajkwa-specific mineralogy, sediment binding phases, or bioavailability (Burton, 2002; MacDonald et al., 2000).

Table 5. Sediment Cu and As compared with freshwater PECs (MacDonald et al., 2000); exceedance indicates screening concern, not formal ecological risk

Analyte	Observed range (mg kg−1)	Mean (mg kg−1)	Freshwater PEC (mg kg−1)	Stations > PEC	Observed/ PEC range
Cu	805.74 - 1,644.79	1,064.81	149	20/20	5.4-11.0×
As	104.62 - 471.55	343.94	33	20/20	3.2-14.3×

Water Cu, As, and Hg were below reporting limits, while sediment Cu and As remained high. Sediments can retain persistent metal signals (Granger et al., 2022; Kolarova & Napiórkowski, 2021; Nazir et al., 2024), although XRF concentrations do not indicate full bioavailability (Luoma, 1983; Rainbow, 2007; Väänänen et al., 2018). Arsenic may also be remobilized under changing redox conditions (Doherty et al., 2021; Lee et al., 2010; Toevs et al., 2006).

Significance of the sediment Cu and As concentrations

All sediment Cu and As concentrations exceeded freshwater PECs, which are screening rather than formal ecological-risk thresholds (MacDonald et al., 2000). These guidelines should not be used as stand-alone regulatory criteria because toxicity depends on site-specific conditions (Burton, 2002). Spatial variability may reflect source proximity, particle sorting, hydrodynamics, and deposition (Cuevas et al., 2023; Granger et al., 2022; Tian et al., 2024). Tailings particles may also be redistributed after deposition (Granger et al., 2022). Differences between Cu and As may reflect distinct mineral or sorption phases (Doherty et al., 2021), while As mobility is influenced by microbial and redox processes (Lee et al., 2010). These mechanisms cannot be resolved from bulk XRF data alone.

Spatial modeling: what the maps can and cannot show

Cross-validation is necessary because smooth interpolation may still perform poorly (Qiao et al., 2018), and sampling density can affect accuracy (Wen et al., 2022). As showed stronger IDW performance (R^2 = 0.965; RMSE = 22.25; MAE = 16.05 mg kg−1) than Cu (R^2 = 0.391; RMSE = 148.73; MAE = 86.10 mg kg−1), requiring greater caution for Cu. Water metals were not interpolated because all observations were non-detects and substitution could create artificial gradients (Helsel, 2006).

Relationship to previous environmental studies in Mimika

The study extends previous work in Mimika through paired water-sediment geochemistry. Mining-related landscape changes have been identified using satellite data

(Alonzo et al., 2016), while tailings-related ecosystem changes have been reported in ModADA (Taberima et al., 2020). Although sources cannot be confirmed, the spatial patterns support future source-apportionment studies. Pollution indices require careful reference selection (Birch, 2023), while enrichment factors can help distinguish lithogenic and anthropogenic contributions (Loska & Wiechuła, 2003).

Strengths and limitations

The study benefits from paired water-sediment sampling, consistent coordinates, censor-aware water-metal interpretation, and cross-validated interpolation. However, single-period sampling and the absence of grain-size, mineralogical, organic-carbon, pore-water, speciation, and sediment Hg data limit mechanistic interpretation of Cu and as patterns. Reproducibility is also constrained by incomplete laboratory QA/QC details, including AAS mode, preservation, instrument, SOPs, standards, blanks, duplicates, and detection limits.

CONCLUSION

The Ajkwa River dataset demonstrates a clear contrast between surface-water and sediment conditions. Surface-water pH and DO remained within the Class III/IV reference ranges, while Cu, As, and Hg were below laboratory reporting limits, indicating no RL-based exceedance of the cited water-quality criteria. In contrast, sediment XRF analysis revealed substantially higher Cu and As concentrations, with pronounced spatial variability along the sampling corridor. IDW cross-validation confirmed markedly different predictive performance between the two analytes, with As showing high spatial stability (R^2 = 0.965; RMSE = 22.25 mg kg−1; MAE = 16.05 mg kg−1), whereas Cu showed lower predictability (R^2 = 0.391; RMSE = 148.73 mg kg−1; MAE = 86.10 mg kg−1). All sediment Cu and As concentrations exceeded freshwater PECs, but only as screening-level indications, not formal ecological risk. The study highlights the value of paired water-sediment data, censor-aware interpretation, and cross-validated spatial modeling. Future studies should include multi-season sampling, hydrological and sediment characteristics, metal speciation, and more complete QA/QC.

ACKNOWLEDGMENT

The authors gratefully acknowledge the financial support provided through the Beginner Lecturer Research (Penelitian Dosen Pemula, PDP) scheme of the Directorate of Research and Community Service (DPPM), Ministry of Higher Education, Science, and Technology of the Republic of Indonesia, with a total research grant of IDR 46,710,000.00. The authors also express their sincere appreciation to PT SUCOFINDO Makassar Branch for conducting Atomic Absorption Spectrophotometry (AAS) analysis of the water samples and to the Mining Engineering Laboratory, Universitas Hasanuddin, for performing X-Ray Fluorescence (XRF) analysis of the sediment samples.

References

Alonzo, M., Van Den Hoek, J., & Ahmed, N. (2016). Capturing coupled riparian and coastal disturbance from industrial mining using cloud-resilient satellite time series analysis. Scientific Reports, 6, Article 35129. https://doi.org/10.1038/srep35129

Birch, G. F. (2023). A review and critical assessment of sedimentary metal indices used in determining the magnitude of anthropogenic change in coastal environments. Science of the Total Environment, 854, Article 158129. https://doi.org/10.1016/j.scitotenv.2022.158129

Burton, G. A., Jr. (2002). Sediment quality criteria in use around the world. Limnology, 3, 65–76. https://doi.org/10.1007/s102010200008

Cuevas, J. G., Faz, A., Martínez-Martínez, S., Gabarrón, M., Beltrá, J. C., Martínez, J., & Acosta, J. A. (2023). Spatial distribution and pollution evaluation in dry riverbeds affected by mine tailings. Environmental Geochemistry and Health, 45(12), 9157–9173. https://doi.org/10.1007/s10653-022-01469-5

Doherty, S., Tighe, M. K., Milan, L. A., Johannessen, B., Mitchell, V., Hamilton, J., Johnston, S. G., & Wilson, S. C. (2021). Long-range spatial variability in sediment associations and solid-phase speciation of antimony and arsenic in a mining-impacted river system. Applied Geochemistry, 135, Article 105112. https://doi.org/10.1016/j.apgeochem.2021.105112

Government of Indonesia. (2021). Government regulation of the Republic of Indonesia No. 22 of 2021 concerning the implementation of environmental protection and management, Appendix VI: National water quality standards.

Granger, B., Laval, B., Vagle, S., Petticrew, E. L., Owens, P. N., & Baldwin, S. A. (2022). Initial distribution and interannual decrease of suspended sediment in a two-basin lake following a massive mine tailings spill: Quesnel Lake, BC, Canada. Water Resources Research, 58, Article e2021WR030574. https://doi.org/10.1029/2021WR030574

Helsel, D. R. (2006). Fabricating data: How substituting values for nondetects can ruin results, and what can

be done about it. Chemosphere, 65(11), 2434–2439. https://doi.org/10.1016/j.chemosphere.2006.04.051

Jewell, D. A., Campbell, L. M., & White, H. P. (2024). An exploration of false positives following multispectral analysis of mine tailings extent. Canadian Journal of Remote Sensing, 50(1), Article 2338357. https://doi.org/10.1080/07038992.2024.2338357

Kolarova, N., & Napiórkowski, P. (2021). Trace elements in aquatic environment: Origin, distribution, assessment and toxicity effect for the aquatic biota. Ecohydrology & Hydrobiology, 21(4), 655–668. https://doi.org/10.1016/j.ecohyd.2021.02.002

Lee, K.-Y., Kim, K.-W., & Kim, S.-O. (2010). Geochemical and microbial effects on the mobilization of arsenic in mine tailing soils. Environmental Geochemistry and Health, 32(1), 31–44. https://doi.org/10.1007/s10653-009-9263-4

Loska, K., & Wiechuła, D. (2003). Application of principal component analysis for the estimation of source of heavy metal contamination in surface sediments from the Rybnik Reservoir. Chemosphere, 51(8), 723–733. https://doi.org/10.1016/S0045-6535(03)00187-5

Luoma, S. N. (1983). Bioavailability of trace metals to aquatic organisms: A review. Science of the Total Environment, 28(1–3), 1–22. https://doi.org/10.1016/S0048-9697(83)80004-7

MacDonald, D. D., Ingersoll, C. G., & Berger, T. A. (2000). Development and evaluation of consensus-based sediment quality guidelines for freshwater ecosystems. Archives of Environmental Contamination and Toxicology, 39(1), 20–31. https://doi.org/10.1007/s002440010075

Nazir, A., Hussain, S. M., Riyaz, M., Kere, Z., Zargar, M. A., & Karun Dev, L. K. (2024). Environmental risk assessment, spatial distribution, and abundance of heavy metals in surface sediments of Dal Lake-Kashmir, India. Environmental Advances, 17, Article 100562. https://doi.org/10.1016/j.envadv.2024.100562

Qiao, P., Lei, M., Yang, S., Yang, J., Guo, G., & Zhou, X. (2018). Comparing ordinary kriging and inverse distance weighting for soil As pollution in Beijing. Environmental Science and Pollution Research, 25(16), 15597–15608. https://doi.org/10.1007/s11356-018-1552-y

Rainbow, P. S. (2007). Trace metal bioaccumulation: Models, metabolic availability and toxicity. Environment International, 33(4), 576–582. https://doi.org/10.1016/j.envint.2006.05.007

Taberima, S., Junaedi, E., Sarwom, R., Lindongi, L. E., & Mulyanto, B. (2020). The acid mine drainage (AMD) impact of tailings and non-tailings on the ecosystem changes in the ModADA sedimentation area, Timika. Journal of Degraded and Mining Lands Management, 7(2), 2085–2094. https://doi.org/10.15243/jdmlm.2020.072.2085

Tian, S., Zhao, Y., Gong, Y., & Wang, G. (2024). Experimental study on tailings deposition distribution pattern and sedimentation characteristics. ACS Omega, 9(17), 19428–19439. https://doi.org/10.1021/acsomega.4c00138

Toevs, G. R., Morra, M. J., Polizzotto, M. L., Strawn, D. G., Bostick, B. C., & Fendorf, S. (2006). Metal(loid) diagenesis in mine-impacted sediments of Lake Coeur d'Alene, Idaho. Environmental Science & Technology, 40(8), 2537–2543. https://doi.org/10.1021/es051781c

U.S. Environmental Protection Agency. (1994a). Method 200.9: Determination of trace elements by stabilized temperature graphite furnace atomic absorption spectrometry (Revision 2.2).

U.S. Environmental Protection Agency. (1994b). Method 245.1: Determination of mercury in water by cold vapor atomic absorption spectrometry (Revision 3.0).

U.S. Environmental Protection Agency. (2007). SW-846 Method 6200: Field portable X-ray fluorescence spectrometry for the determination of elemental concentrations in soil and sediment.

Väänänen, K., Leppänen, M. T., Chen, X., & Akkanen, J. (2018). Metal bioavailability in ecological risk assessment of freshwater ecosystems: From science to environmental management. Ecotoxicology and Environmental Safety, 147, 430–446. https://doi.org/10.1016/j.ecoenv.2017.08.064

Wen, L., Zhang, L., Bai, J., Wang, Y., Wei, Z., & Liu, H. (2022). Optimizing spatial interpolation method and sampling number for predicting cadmium distribution in the largest shallow lake of North China. Chemosphere, 309, Article 136789. https://doi.org/10.1016/j.chemosphere.2022.136789

Yang, Y., & Jia, M. (2024). 3D spatial interpolation of soil heavy metals by combining kriging with depth function trend model. Journal of Hazardous Materials, 461, Article 132571. https://doi.org/10.1016/j.jhazmat.2023.132571